



# A novel infectious hematopoietic necrosis virus (IHNV) isolated from white-spotted charr (*Salvelinus leucomaenis*) is moderately virulent to rainbow trout (*Oncorhynchus mykiss*)

Chunyan Guan<sup>a,c</sup>, Jingzhuang Zhao<sup>a,b</sup>, Yizhi Shao<sup>a,b</sup>, Tongyan Lu<sup>a,b</sup>, Liming Xu<sup>a,b,\*</sup>

<sup>a</sup> Department of Aquatic Animal Diseases and Control, Heilongjiang River Fisheries Research Institute, Chinese Academy of Fishery Sciences, Harbin 150070, China

<sup>b</sup> Key Laboratory of Aquatic Animal Diseases and Immune Technology of Heilongjiang Province, Harbin 150070, China

<sup>c</sup> University of Dalian Ocean University, College of Fisheries and Life Sciences, Dalian, China

## ARTICLE INFO

### Keywords:

White-spotted charr  
Rainbow trout  
IHNV  
J genogroup  
Pathogenicity

## ABSTRACT

J genogroup infectious hematopoietic necrosis virus (IHNV) is mostly isolated from rainbow trout (*Oncorhynchus mykiss*). In this study, a novel IHNV strain, designated as H202217, was isolated from diseased white-spotted charr (*Salvelinus leucomaenis*). The phylogenetic analysis showed that the H202217 strain had the closest relationship with other Chinese J genogroup IHNV strains isolated from rainbow trout. *In vitro* proliferation experiments showed that the H202217 strain had lower titer but similar immunogenicity with the Sn1203 strain, a reference strain isolated from rainbow trout. In the artificial infection of white-spotted charr, the H202217 strain showed low virulence, and caused a cumulative percentage of mortality (CPM) of 15 %, which was higher than the CPM of 7.5 % caused by the Sn1203 strain. While challenged in rainbow trout, the H202217 strain caused moderate CPM of 22 %, lower than that of 46 % caused by the Sn1203 strain. In addition, the viral loads of the H202217 strain were higher than those of Sn1203 strain in white-spotted charr, while it was the opposite in the rainbow trout. These results suggest that the H202217 strain has better fitness with white-spotted charr and lost partial virulence to rainbow trout compared with the rainbow trout sourced IHNV Sn1203 strain, and which has potential use to reveal the IHNV virulence evolution accompanied with host jump in the future.

## 1. Introduction

Infectious hematopoietic necrosis (IHN) disease, caused by infectious hematopoietic necrosis virus (IHNV), is an acute disease of salmonids with high mortality, approaching 100 % in some conditions, leading to huge economic losses to the salmon and trout industry worldwide (Dixon et al., 2016). IHNV is a single-stranded negative-sense RNA virus, classified in the family *Rhabdoviridae*, the genus *Novirhabdovirus*, and mainly composed of five structural proteins nucleoprotein (N), phosphoprotein (P), matrix protein (M), glycoprotein (G), RNA-dependent RNA polymerase (L), and a non-structural protein (NV) (Xu et al., 2019). According to the phylogenetic tree analysis of the IHNV G gene, IHNV was divided into five genogroups: U, L, M, E, and J, providing a theoretical basis for insight into its molecular epidemiology and evolutionary characteristics (Enzmann et al., 2010; He et al., 2021; Kurath et al., 2003). The U, L, and M genogroups were mainly endemic in North

America, the E genogroup was predominantly popular in Europe, and the J genogroup evolved from the U genogroup was dominant in the Asian countries.

IHNV was initially found in sockeye salmon (*Oncorhynchus nerka*) in Washington and Oregon in the 1950s. For now, it has been identified in many salmonid species, mainly rainbow or steelhead trout (*Oncorhynchus mykiss*), Chinook (*O. tshawytscha*), sockeye (*O. nerka*), chum (*O. keta*), amago (*O. rhodurus*), masou (*O. masou*), coho (*O. kisutch*), and Atlantic salmon (*Salmo salar*). IHNV has also occasionally been found to be infected in the wild or shown to be susceptible by a natural route of infection in other salmonids including brown trout (*Salmo trutta*), cutthroat trout (*O. clarki*), and fish within the genus *Salvelinus*, such as brook trout (*S. fontinalis*), Arctic charr (*S. alpinus*), lake trout (*S. namaycush*) and white-spotted charr (*S. leucomaenis*) (OIE, 2021). Different genogroups of IHNV adapt to different susceptible fish species, resulting in differences in infectivity and lethality among various fish

\* Corresponding author at: Department of Aquatic Animal Diseases and Control, Heilongjiang River Fisheries Research Institute, Chinese Academy of Fishery Sciences, Harbin, China.

E-mail address: [lmxu0917@163.com](mailto:lmxu0917@163.com) (L. Xu).

<https://doi.org/10.1016/j.aquaculture.2025.742839>

Received 12 March 2025; Received in revised form 8 May 2025; Accepted 9 June 2025

Available online 10 June 2025

0044-8486/© 2025 Elsevier B.V. All rights are reserved, including those for text and data mining, AI training, and similar technologies.

species (Garver et al., 2006; Hoffmann et al., 2005). Among the five genogroups, U and L were usually found in sockeye salmon and Chinook salmon, respectively, while E, J, and M were mainly found in rainbow trout (Breyta et al., 2016; Kurath et al., 2003). In this study, we isolated and characterized a novel J genogroup IHN strain from diseased white-spotted charr, and *in vivo* and *in vitro* tests were performed to compare the virulence between the white-spotted charr resourced IHN strain and a rainbow trout-resourced IHN strain.

## 2. Materials and methods

### 2.1. Cell lines, virus strains, and fish

The *Epithelioma papulosum cyprini* (EPC) and *Chinook salmon embryonic* (CHSE-214) cell lines, as well as the *Rainbow trout gonad-2* (RTG-2), were generously provided by Prof. Zeng from the Yangtze River Fisheries Research Institute. All the cells were cultured in the Minimum Essential Medium (MEM, cat. no. 1109500; Gibco, Grand Island, NY, USA) supplemented with 10 % fetal bovine serum (FBS, cat. no. FB25015; Gibco) at 20 °C. The EPC and CHSE-214 cell lines were used for virus isolation. In the virus isolation experiment, the cells were transferred to MEM supplemented with 2 % FBS at 15 °C. The J genogroup IHN Sn1203 strain isolated from rainbow trout (*Oncorhynchus mykiss*) was used in this study as a reference virus to test the virulence of the newly isolated IHN strain, and the titer of the Sn1203 strain in the EPC cell lines is  $10^{7.5}$  TCID<sub>50</sub>/0.1 mL.

Specific pathogen-free rainbow trout ( $7.5 \pm 1.7$  g) were purchased from the Agricultural Marine Company (Benxi, China) and Diamond Heart Lake (Mudanjiang, China), and their eyed eggs were imported from Spain, respectively. The white-spotted charr ( $8.2 \pm 1.7$  g) was purchased from a local farm in the Northeast of China. All fish were used for virus challenge experiments.

### 2.2. Isolation and characterization of virus

The organs (liver, spleen, and head kidney) were collected from moribund white-spotted charr (30–40 cm) and homogenized in Phosphate Buffered Solution (PBS, cat. no. BL302A; BioSharp®, Hefei, China). After centrifuged at 12000 rpm for 15 min at 4 °C, the tissue supernatant was 10-fold diluted with MEM medium (2 % FBS), and 1 mL of the supernatant was inoculated into monolayer EPC cells and CHSE-214 cells, respectively. The cells were daily observed for cytopathic effects (CPE) during the following 7 d. If no CPE was observed, the cells were frozen and thawed once and inoculated on new monolayer cells for another 7 days of observation. Cells that showed CPE were further identified by RNA extraction followed by PCR by using the PrimeScript™ One-Step RT-PCR Kit Ver.2 (cat. no. RR057A; Takara, Shiga, Japan). The amplification procedure was as follows: 50 °C for 30 min, 94 °C for 4 min, 94 °C for 30 s, 55 °C for 30 s, 72 °C for 2 min, 72 °C for 10 min, final incubation at 4 °C, and the cycles was 30.

In this study, IHN, infectious pancreatic necrosis virus (IPNV) (Duan et al., 2021), and viral hemorrhagic septicemia virus (VHSV) were detected with previously used primers (Xu et al., 2020).

### 2.3. Genome sequencing and phylogenetic analyses

An IHN strain was isolated from the diseased white-spotted charr, designated as the H202217, and the complete genome of the virus strain was amplified by using six pairs of overlapped primers that cover the entire IHN genome. Phylogenetic trees were constructed based on N, G, and NV open reading frame (ORF) by using MEGA 6.0. Phylogenetic trees were constructed using the Clustal W multiple alignment and using the neighbor-joining method with 1000 bootstrap replicates (Felsenstein, 1985; Saitou and Nei, 1987). Primers for amplification of IHN genome was listed in **Supplementary Table S1**.

### 2.4. Indirect immunofluorescence antibody test (IFAT)

Monolayer cells of CHSE-214 were inoculated with 10  $\mu$ L of IHN original suspension and cultured at 15 °C. At 36 h post-infection (h.p.i), the supernatant is discarded, and monolayer cells were fixed, blocked, and subsequently incubated with the primary polyclonal antibody (Xu et al., 2020) and the secondary monoclonal antibody (Cy3-tagged goat anti-rabbit IgG antibody) (cat. no. BD9724; Biodragon, Red fluorescence). The cell nucleus was stained with DAPI staining solution (cat. no. C1006; Beyotime Biotechnology, Shanghai, China) for 5 min. The polyclonal antibody was made by our laboratory and was used to label the IHN G protein. After incubation, cells were washed three times with PBS and observed by a confocal fluorescence microscope (Leica, Wetzlar, Germany).

### 2.5. Virus growth kinetics in three cell lines

The dynamic growth status of IHN isolates was tested by using EPC, CHSE-214, and RTG-2 cell lines, respectively. Monolayer cells of EPC were inoculated with 100 TCID<sub>50</sub>/0.1 mL of the H202217 and Sn1203 isolate, respectively, and cultured with MEM (2 % FBS) at 15 °C. 200  $\mu$ L supernatants were collected each day during the following 7 d for measuring viral titers. After collection of the supernatant, the remaining virus-inoculated cells were added 200  $\mu$ L of MEM (2 % FBS). The supernatant was 10-fold serially diluted ( $10^{-1}$ – $10^{-9}$ ) and inoculated into EPC cells in a 96-well plate. The 96-well plate of EPC cells was observed at 7 d.p.i. and viral titer was calculated by the 50 % tissue culture infective dose (TCID<sub>50</sub>/0.1 mL) according to the Reed and Muench method. Dynamic viral titers in CHSE-214 cells and RTG-2 cells were determined by using the same protocol, but the inoculation dosage was  $10^{5.5}$  TCID<sub>50</sub>/0.1 mL and  $10^4$  TCID<sub>50</sub>/0.1 mL, respectively.

### 2.6. Virus challenge of white-spotted charr

The white-spotted charr ( $n = 80$ ,  $8.2 \pm 1.7$  g) was intraperitoneally injected with 50  $\mu$ L  $10^{6.5}$  TCID<sub>50</sub>/0.1 mL of the H202217 and IHN Sn1203, respectively, with 80 fish in each group, of which 40 were used for mortality statistics, and the other 40 fish were sampled for viral loads determination. The liver, spleen, head kidney, brain, gills, and intestines of alive white-spotted charr ( $n = 4$ ) were collected at 1, 3, 7, and 14 days post-challenge (d.p.c), and RNA was extracted by using Trizol reagent (cat. no. 15596026; Invitrogen, Carlsbad, CA, USA). The synthesis of cDNA was generated by using the HiScriptIIQ RT SuperMix (cat. no. R223-01; Vazyme, Nanjing, China), and the relative expression level of the IHN G gene in the tissues was measured by using Quantitative Real-time polymerase chain reaction (qPCR) with SYBR Green (cat. no. Q711-02; Vazyme) on LightCycler® 96 detection System (Roche, Switzerland). The  $\beta$ -actin was the reference gene (Xu et al., 2020). Fold changes of the IHN G gene expression levels in different tissues were calculated according to the  $2^{-\Delta\Delta C_t}$  method. The cumulative percentage mortality (CPM) was recorded for 21 days and tissues of dead fish were used to identify the presence of IHN.

### 2.7. Virus challenge of rainbow trout

Rainbow trout ( $n = 80$ ,  $7.5 \pm 1.7$  g) was intraperitoneally injected with 100 TCID<sub>50</sub>/0.1 mL of the H202217 strain and the Sn1203 strain, of which 40 fish per group were used for CPM determination during the following 21 days, and the other 40 fish were used for viral loads determination. The tissues of alive rainbow trout ( $n = 4$ ) at 1, 3, 7, 14, 21 d.p.c and dead fish were collected for measuring viral loads. The collected tissues, including liver, spleen, head and kidney, brain, gills, and intestines, were ground and then diluted with PBS at a ratio of 1:5 (w/v), respectively, and were centrifuged at 12000 g for 15 min at 4 °C. The filtered tissue supernatant was 10-fold serially diluted ( $10^{-1}$ – $10^{-9}$ ) and was inoculated into EPC monolayers cultured in 96-well plates. The

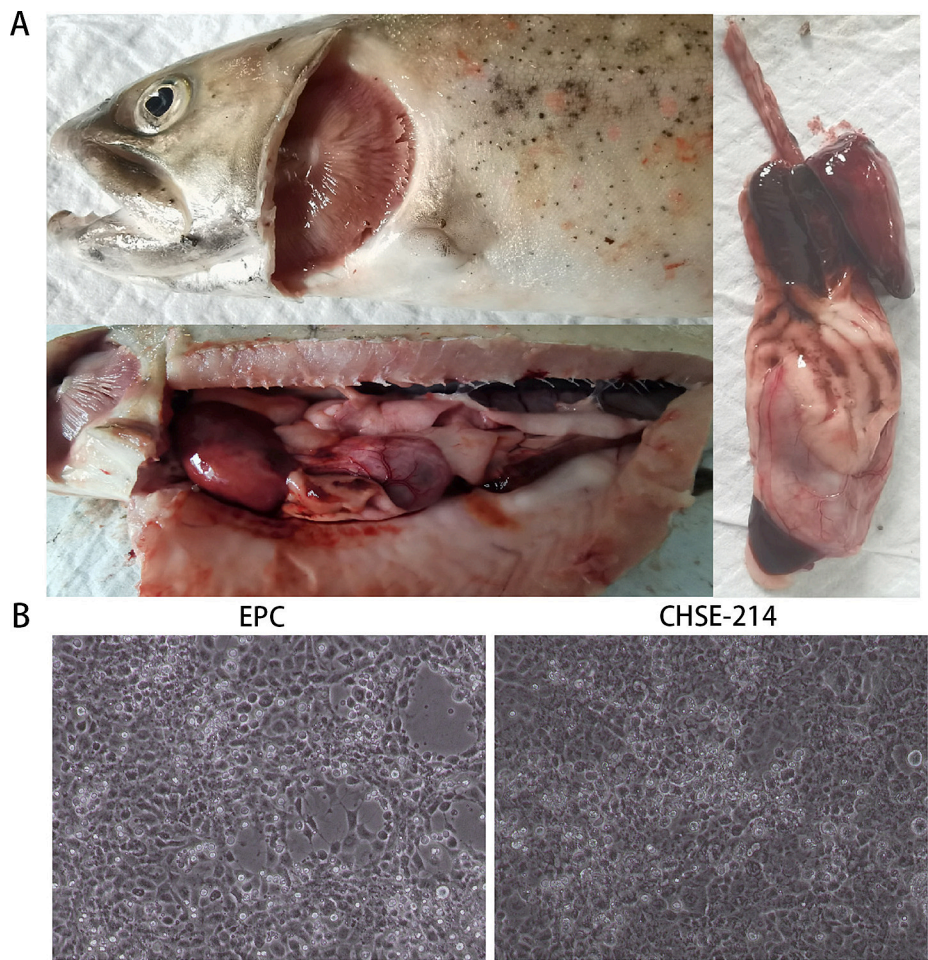


Fig. 1. Clinical features of the diseased white-spotted charr and CPE in the EPC and CHSE-214 cell lines.

inoculated cell was cultured at 15 °C for 7 days and the viral titer was determined using the Reed-Muench method. Three parallel experiments were independently measured on viral loads at each time point. Mean-time, the relative expression levels of the IHNV *G* gene in tissues were determined by RT-qPCR as described above.

2.8. Statistical analysis

Experimental data were presented as mean ± standard deviation (SD) and statistically analyzed. One-way analysis of variance (ANOVA) in SPASS 13.0 was used to detect the significance of the experiment in different experimental groups, and Prims Graphpad 9 was used for charting.

3. Results

3.1. Virus isolation

The diseased white-spotted charr showed black spots on the skin, gill anemia, and severe hemorrhage of the liver and digestive tract (Fig. 1A). The accumulation mortality of the fish was approximately 25 %. No parasites were observed on the skin or the gill. After the inoculation of tissue supernatant into EPC and CHSE-214 cells, CPE was observed in both cell lines (Fig. 1B). One-step RT-PCR showed that the specific band was only observed by using IHNV specific primers, and the results for the other two viruses (VHSV and IPNV) were tested negative. The virus isolated from the diseased white-spotted charr sample was named IHNV H202217.

**Table 1**  
Amino acid comparison between IHNV H202217 and Sn1203 strains.

Open reading frame	Sites of distinct amino acids	Amino acids Sn1203/H202217
N	91	D/G
	192	I/V
P	43	G/D
	40	K/R
M	135	N/T
	170	R/K
	192	G/E
	134	A/S
	177	T/A
	275	S/A
G	286	E/K
	424	S/G
	435	A/V
	454	D/A
	501	M/T
	59	K/Q
NV	102	L/P
	66	T/A
	80	V/E
	164	E/V
	241	K/Q
	314	F/S
L	714	T/A
	724	L/M
	1317	C/W
	1492	A/T
	1519	T/A
	1957	K/R



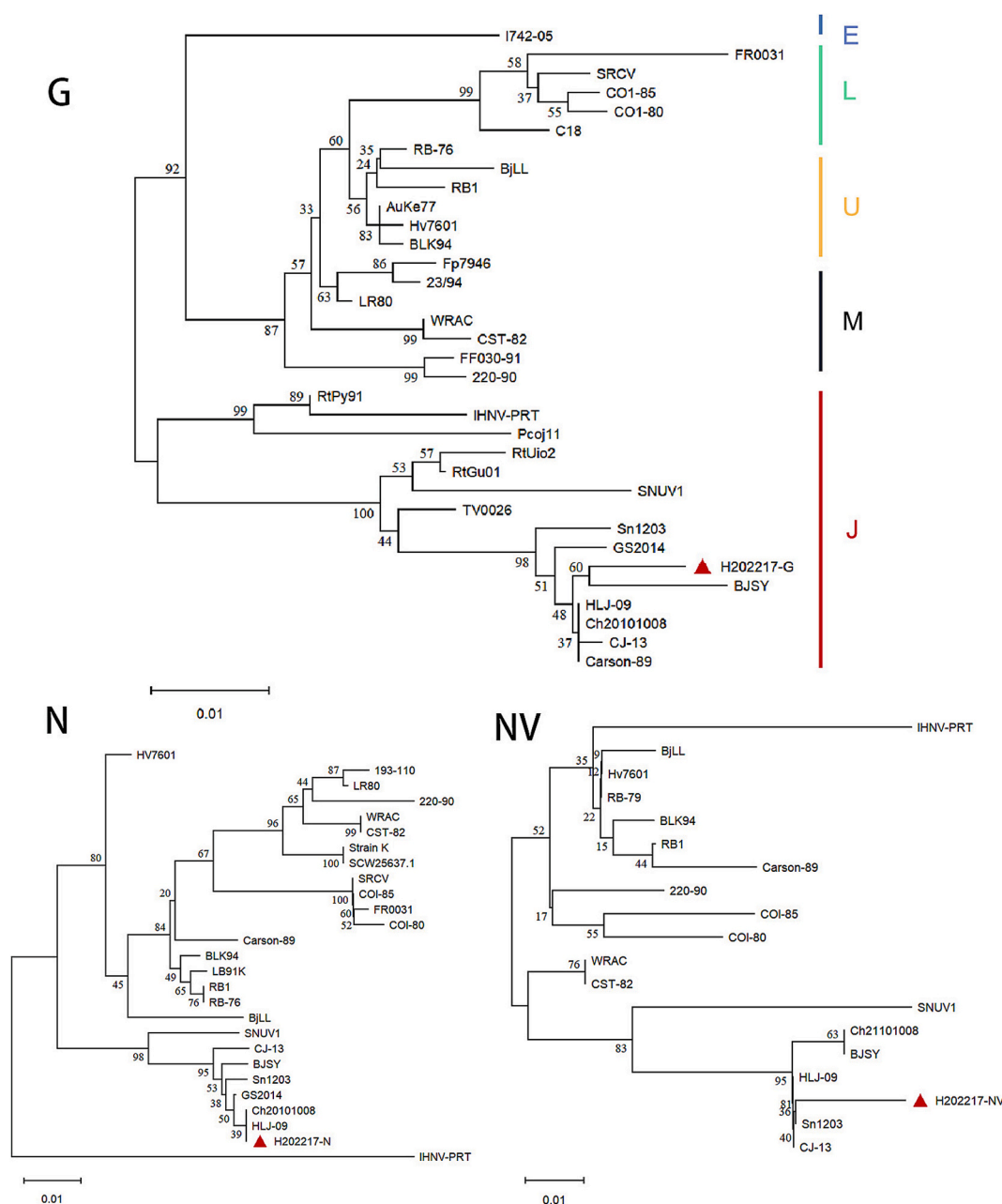


**Fig. 2.** Phylogenetic trees of the IHN H202217. Phylogenetic analyses were performed by using MEGA 6.0 and Clustal W multiple alignment algorithm. The evolutionary distances were measured in the units of the number of amino acid substitutions at each site and the scale was 0.01.

### 3.2. Homology analysis and phylogenetic tree of the IHN H202217

The entire genome of the IHN H202217 was amplified and sequenced. Compared with the genome of IHN Sn1203, the H202217 had a total of 29 amino acid mutations (Table 1). Notably, most amino acid mutations occurred in the G and L proteins. Phylogenetic trees were constructed based on G, N, and NV ORFs of the IHN H202217. The IHN H202217 was consistently clustered in the J genogroup with other Chinese IHN strains (Fig. 2). The G, N, and NV genes of H202217 strain were mostly close to the HLJ-09 strain, BJSY strain, and the Sn1203 strain, respectively (Fig. 2).

### 3.3. IHN H202217 determined by IFAT

To compare the antigenicity of the G protein of the IHN H202217 with that of the IHN Sn1203, the IHN H202217 was determined by

IFAT with G polyclonal antibody against the IHN Sn1203. The results showed that the IHN H202217 could cause typical CPE at 36 h.p.i and the G protein of the H202217 could be recognized by the antibody specific to the G protein of IHN Sn1203. Specific fluorescent signal was observed in both the virus strains infected cells, and no difference in signal intensity was observed between cells infected with the H202217 strain and the Sn1203 strain. The result suggested that the IHN H202217 had similar G protein epitopes to that of the IHN Sn1203 (Fig. 3).

### 3.4. Viral replication kinetics in cell lines

Viral titers of the both IHN strains reached the peak of the logarithmic phase at 5 d.p.i. in each of the three cell lines and then entered a plateau phase (Fig. 4A-C). As shown in Fig. 4D, the viral titers in EPC and CHSE-214 of the IHN H202217 at 7 d.p.i. were  $10^{6.67}$  and  $10^{5.78}$



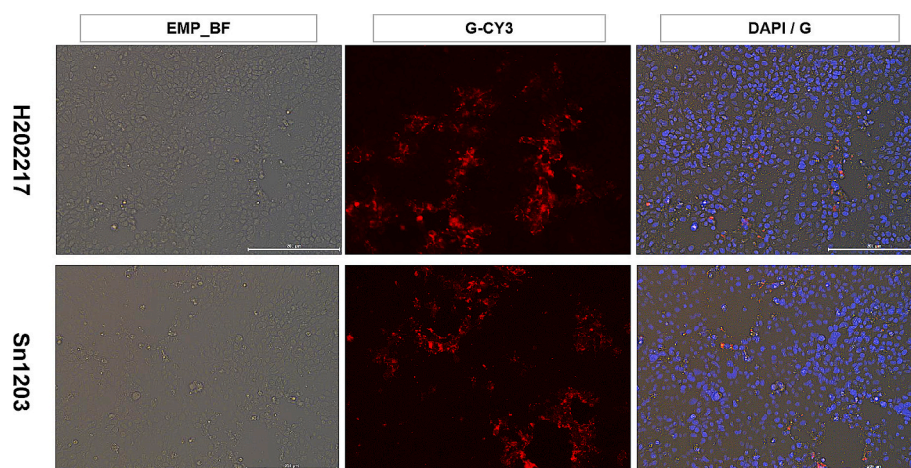


**Fig. 3.** Immunogenicity analysis of the IHN H202217. The image indicates the existence of the viral G protein (red) and cell nucleus (blue). (For interpretation of the references to colour in this figure legend, the reader is referred to the web version of this article.)

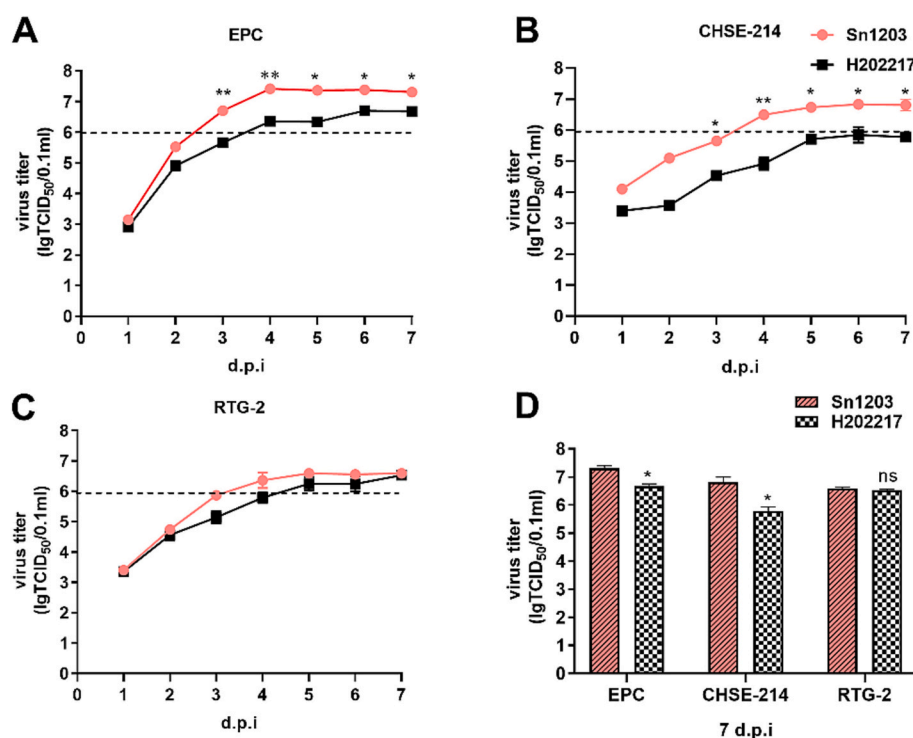


**Fig. 4.** *In vitro* multiplication properties of the IHN H202217. The IHN Sn1203 was used as a reference strain. Data represent three independent experiments (mean  $\pm$  SD). \*  $p < 0.05$ ; \*\*  $p < 0.01$ .

TCID<sub>50</sub>/ 0.1 mL, and both were significantly lower than those of the IHN Sn1203, which were  $10^{7.31}$  and  $10^{6.81}$ , respectively ( $p < 0.05$ ). However, the IHN H202217 had a similar viral titer to the IHN Sn1203 in the RTG-2 cell lines (Fig. 4D) ( $p > 0.05$ ). Final titer of the IHN H202217 in the CHSE-214 was significantly lower than that of the IHN Sn1203 ( $p < 0.05$ ), and were  $10^{5.77}$  and  $10^{6.81}$ , respectively ( $p < 0.05$ ). The viral titers of the both IHN strains in EPC cell lines were higher than those in the CHSE-214 cell lines, and the lowest viral titers were observed in the RTG-2 cell lines.

### 3.5. Pathogenicity and proliferative properties of the H202217 in white-spotted charr

To further determine the pathogenicity of the virus strain of

H202217, artificial infection was performed by challenging white-spotted charr ( $n = 30$ ) with the IHN H202217 and IHN Sn1203, and the mortality and viral loads in the maintained fish were measured. The results showed that the CPM of white-spotted charr caused by H202217 was 15 %, higher than the 7.5 % caused by Sn1203 (Fig. 5A). The relative expression level of the IHN G gene showed a fluctuating change in the alive fish, and those in the fish infected with the H202217 strain were significantly higher than those in the fish infected with the Sn1203 strain in the vast majority of tissues (Fig. 5B) ( $p < 0.05$ ). The expression levels of the IHN G gene reached high points at 3 d.p.c and 7 d.p.c in most tissues except gills, and those of the H202217 strain were significantly higher than those of the Sn1203 strain ( $p < 0.05$ ). At 5 d.p.c, the relative expression levels of the IHN G gene of the H202217 strain in the liver and the intestines were significantly lower than those

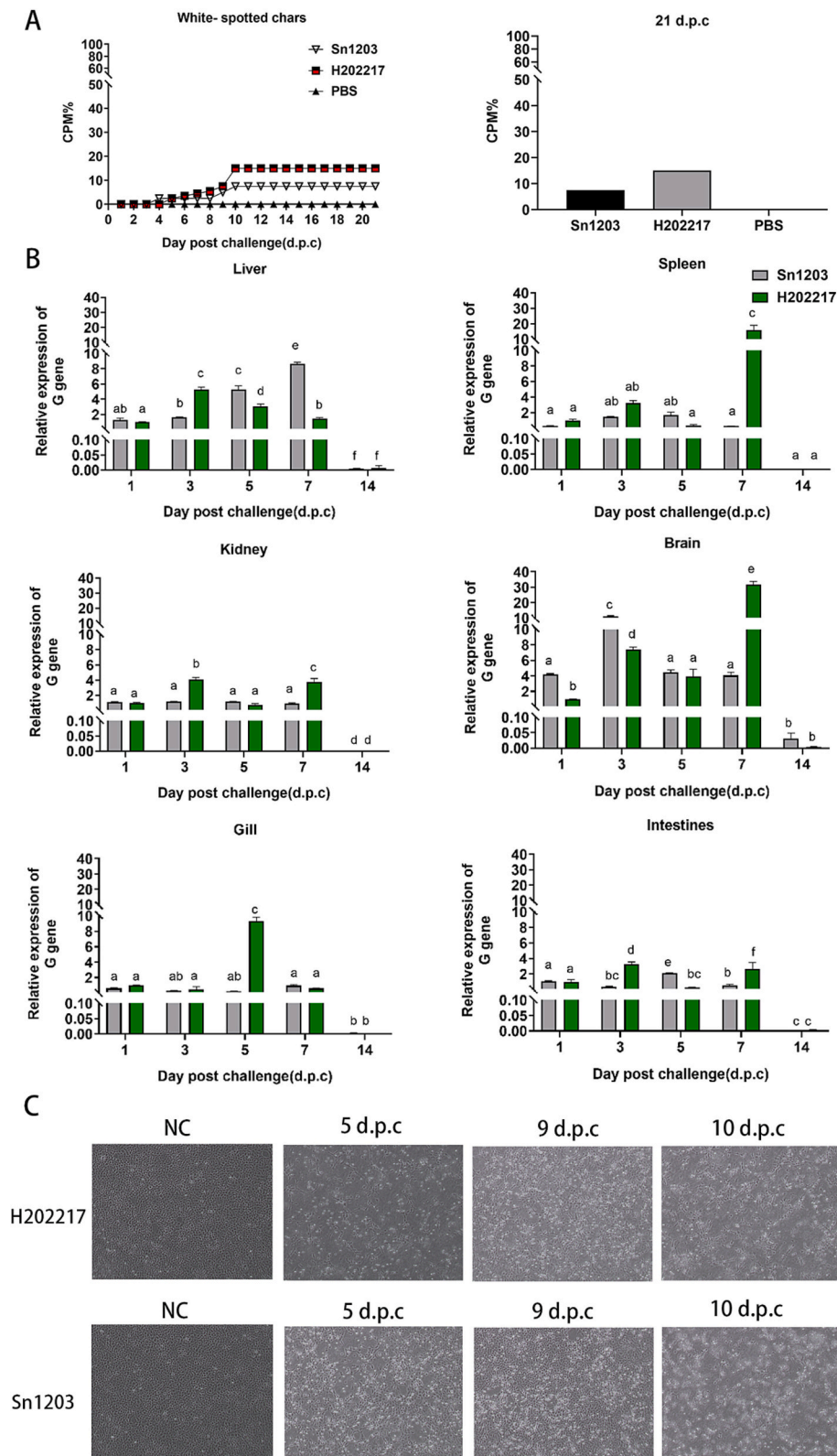


**Fig. 5.** The white-spotted charr ( $8.2 \pm 1.7$  g) was challenged with the IHNV H202217 and IHNV Sn1203. The CPM (A) was recorded and *G* gene expression of IHNV in alive fish (B) was determined. The relative expression level of the *G* gene in H202217 was defined as 1 in each tissue collected at 1 d.p.c. (C) Tissues from dead fish on different days post-challenge were used for virus isolation and the extent of cytopath appeared at 4 d.p.i. Different letters indicated significant differences ( $p < 0.05$ ).

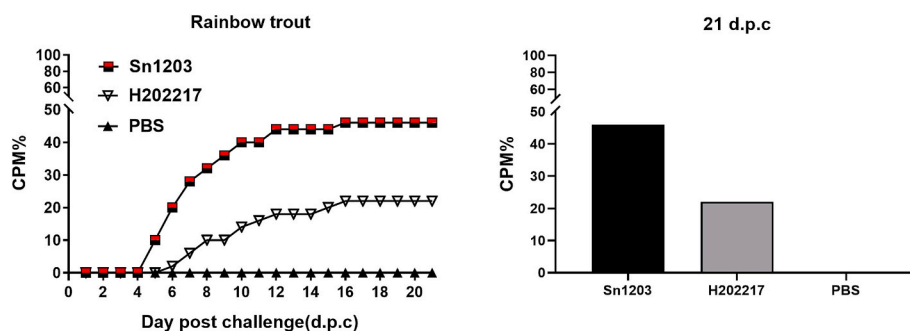


Fig. 6. The cumulative mortality (CPM) of rainbow trout ( $7.5 \pm 1.7$  g) challenged with IHN H202217 and IHN Sn1203.

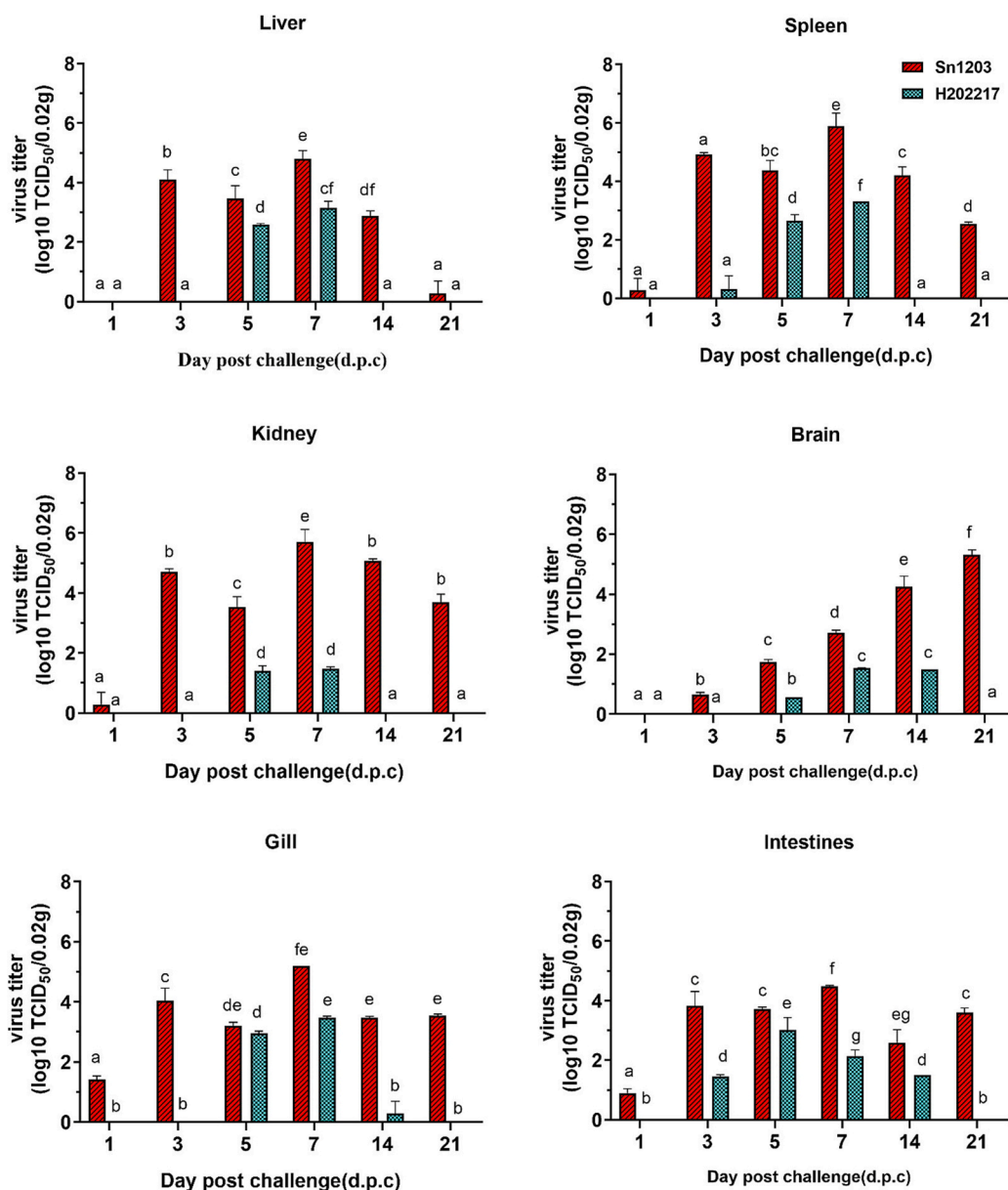


Fig. 7. The viral titers in alive rainbow trout ( $7.5 \pm 1.7$  g) challenged with IHN H202217 or IHN Sn1203. Different letters indicated significant differences ( $p < 0.05$ ).

of the Sn1203 strain, while it was the opposite in the gills ( $p < 0.05$ ). The IHN *G* genes of the two virus strains were almost undetectable at 14 d. p.c. The white-spotted charr infected with either the Sn1203 strain or

the H202217 strain, died at 5, 9, 10 d.p.c and the tissue supernatant from the dead fish caused obvious typical CPE at 4 d.p.i. in the EPC cell lines (Fig. 5C).



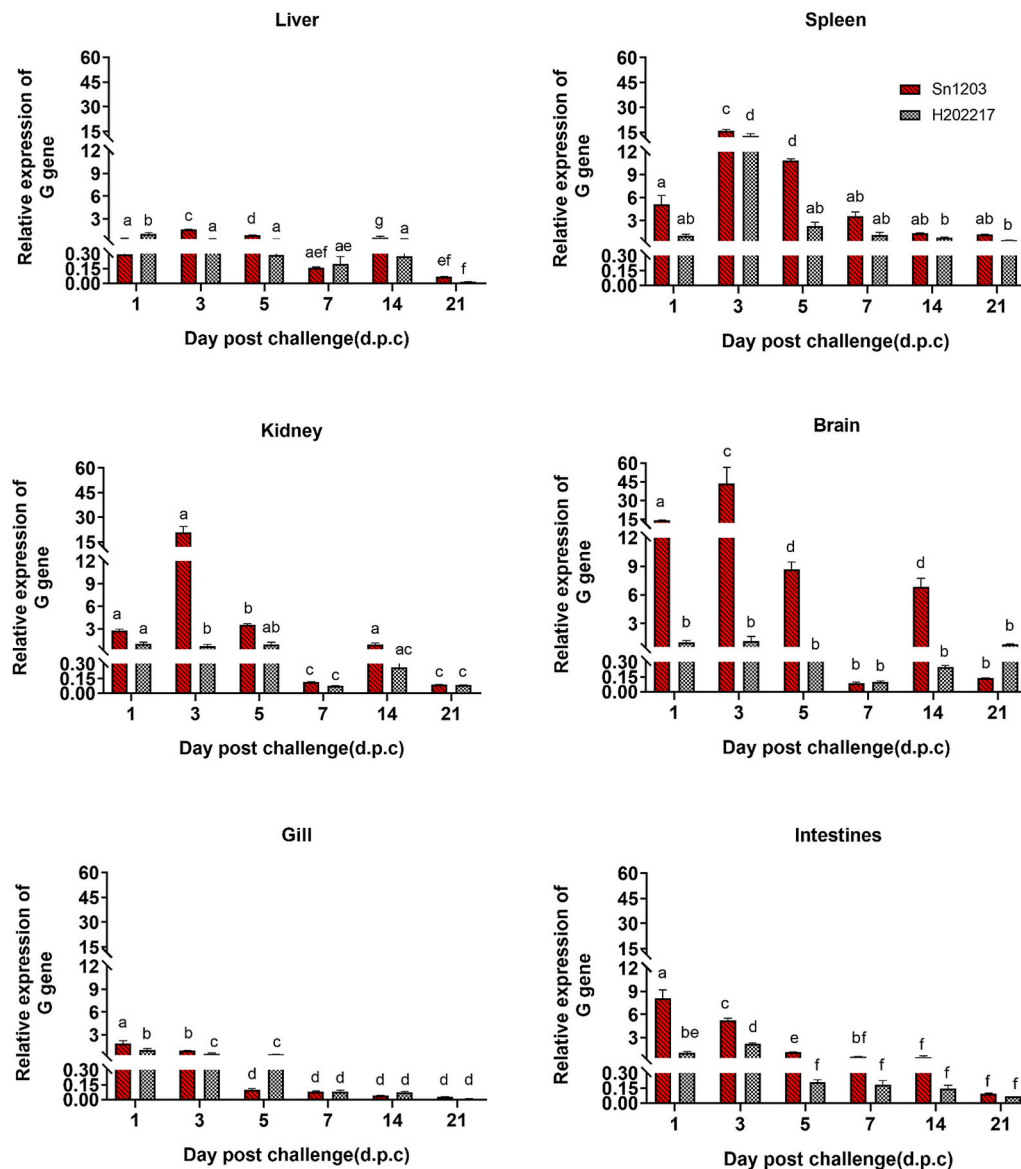


Fig. 8. The viral loads in alive rainbow trout ( $7.5 \pm 1.7$  g) challenged with IHN H202217 or IHN Sn1203. The relative expression level of the IHN *G* gene in the H202217 strain was defined as 1 in different tissues at 1 d.p.c. Different letters indicated significant differences ( $p < 0.05$ ).

### 3.6. Pathogenicity and proliferative properties of H202217 in rainbow trout

Challenged fish began to die at 6 d.p.c and reached a peak of death at 16 d.p.c. The CPM in the H202217 group and Sn1203 group were 22 % and 46 %, respectively (Fig. 6). IHN was quantified in alive rainbow trout ( $7.5 \pm 1.7$  g) by using virus titration and RT-qPCR at 1, 3, 5, 7, 14, and 21 d.p.c. Viral titers of Sn1203 were significantly higher than those of H202217 in the most tissues at 3, 5, 7, 14, 21 d.p.c ( $p < 0.05$ ), while there was no significant difference in the liver at 21 d.p.c and gills at 5 d.p.c ( $p > 0.05$ ; Fig. 7). In the most tissues, viral titers of Sn1203 strains reached a peak of about  $10^5$  TCID<sub>50</sub>/0.02 g at 7 d.p.c, while in each tissue, the viral titers of the H202217 strain were below  $10^5$  TCID<sub>50</sub>/0.02 g (Fig. 7). The IHN *G* gene expression level of both strains reached the highest at 3 d.p.c, except for Sn1203 in intestines at 1 d.p.c (Fig. 8). The IHN *G* gene expression levels of Sn1203 were remarkably higher than those of H202217 in the most tissues at 3, 5 d.p.c ( $p < 0.05$ ), except for in gill at 5 d.p.c. At 7, 14, 21 d.p.c, the IHN *G* gene expression level decreased and there was no significant difference between the Sn1203 group and the H202217 group ( $p > 0.05$ ), except for liver and brain at 14

d.p.c ( $p < 0.05$ ).

IHN was also quantified in the dead rainbow trout by using virus titration and RT-qPCR at 6, 7, 8, 10, and 12 d.p.c. In the most tested tissues from different time points, the viral titers and IHN *G* gene expression levels of the Sn1203 strain in the dead rainbow trout were significantly higher than that of the H202217 strain (Fig. 9 and Fig. 10) ( $p < 0.05$ ). The IHN viral titers were higher in the liver, spleen, kidney, and gills of the dead rainbow trout, the highest viral titer of the Sn1203 strain was close to  $10^6$  TCID<sub>50</sub>/0.02 g and that of the H202217 strain was approximately  $10^5$  TCID<sub>50</sub>/0.02 g (Fig. 9). The IHN *G* gene expression levels of the Sn1203 in the spleen and intestine of the dead fish were significantly higher than the H202217 strain in the spleen and intestines at 6, 7, and 12 d.p.c (Fig. 10) ( $p < 0.05$ ). In the brain, the *G* gene expression levels of the Sn1203 strain reached the highest point at 6 d.p.c and was gradually decreased, and the Sn1203 group was significantly higher than that in the H202217 group ( $p < 0.05$ ).

## 4. Discussion

IHN is an important pathogen that mainly threatens salmonids,

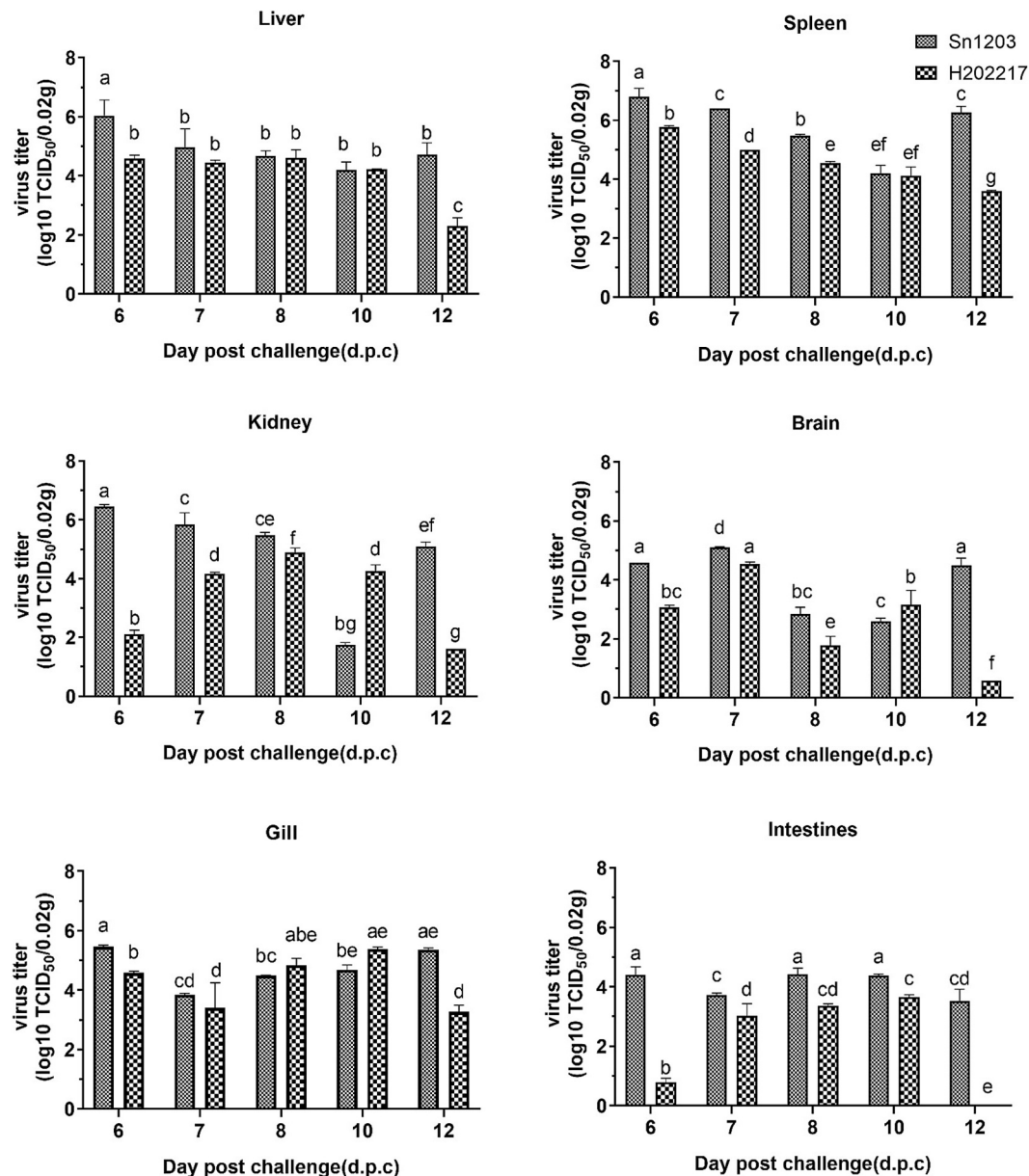


**Fig. 9.** The viral titers in the dead rainbow trout ( $7.5 \pm 1.7$  g) challenged with IHN H202217 or IHN Sn1203. Different letters indicated significant differences ( $p < 0.05$ ).

especially juvenile fish. Different genogroups of IHN adapt to different susceptible fish species, resulting in differences in infectivity and lethality among various fish species (Garver et al., 2006; Hoffmann et al., 2005). Among the five genogroups, U and L were usually found in sockeye salmon and Chinook salmon, respectively, while E, J, and M mainly infect rainbow trout (Breyta et al., 2016; Kurath et al., 2003). Up to now, four species of the genus *salvelinus* have been listed to be susceptible to IHN by OIE (OIE, 2021), among which the susceptibility of brook trout, lake trout, and Arctic charr have been studied by artificial infection, while white-spotted charr was only been found to be infected in the field in Japan (Bootland et al., 1994; Follett et al., 1997; Jia et al., 2013; McAllister et al., 2000).

J genogroup IHN was originally found in Japan, and which was evolved from U genogroup IHN. It had been reported that IHN was imported to China through the contaminated eggs of rainbow trout from Japan in the 1980s (Jia et al., 2014; Niu and Zhao, 1988), and most of the Chinese IHN strains isolated from rainbow trout belonged to the J genogroup, except for one U genogroup strain and one M genogroup

strain (Huo et al., 2022; Jia et al., 2018). The dominant host of Chinese IHN isolates is rainbow trout. The fish farm where the IHN strain was isolated raised several salmonid fish and IHN strains were only observed from fish of the genus *Oncorhynchus*, such as rainbow trout, golden rainbow trout, masou, etc. In this study, we first isolated a novel IHN strain from white-spotted charr in this farm, and it clustered in the J genogroup with other Chinese IHN strains isolated from rainbow trout. Fish in this farm share the same flow-through water, which might provide the environment for the IHN jump from rainbow trout to white-spotted charr.

A similar host jumping had occurred on VHSV, a virus of the same genus as IHN. In the 1950s, VHSV caused high mortality of freshwater rainbow trout in European fish farms, while before that it was reported to mainly infect marine species (Vakharia et al., 2019). The process of infecting hosts that were previously unable to be infected by VHSV was described as host jumping of VHSV during its evolution, and VHSV also subsequently occurred in Northern Europe (Dale et al., 2009; Einer-Jensen et al., 2004; Raja-Halli et al., 2006). Therefore, IHN infection of

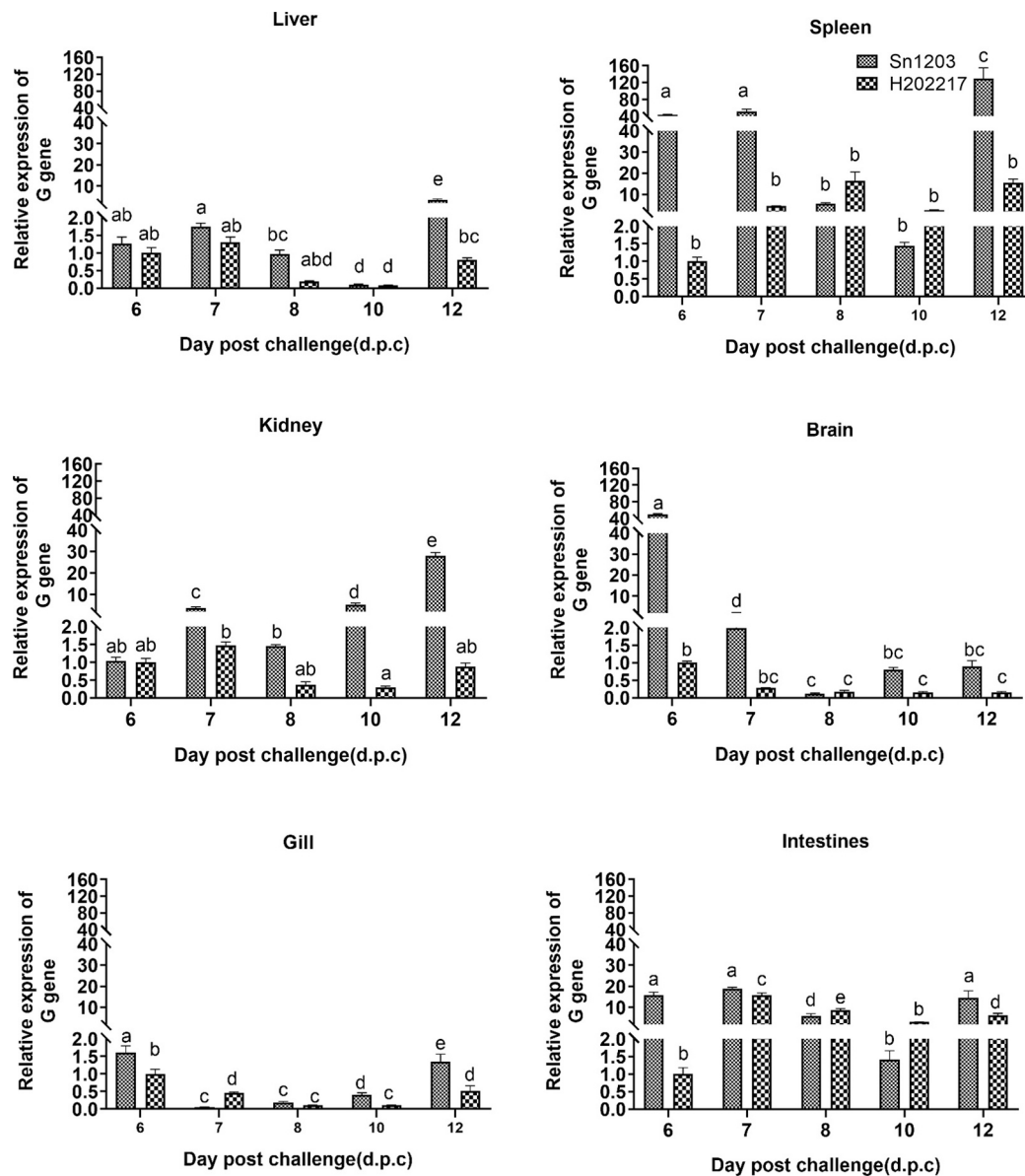


**Fig. 10.** The viral loads in the dead rainbow trout ( $7.5 \pm 1.7$  g) challenged with IHN H202217 or IHN Sn1203. The expression level of the IHN G gene of the H202217 strain was defined as 1 in different tissues at 1 d.p.c. Different letters indicated significant differences ( $p < 0.05$ ).

white-spotted charr may be driven by the evolution of host adaptation and specificity of the virus itself as in previous studies (Pérez et al., 2020; Tan et al., 2024; Wargo et al., 2010).

Viral fitness, the relative ability of a virus to produce infectious offspring in a specific environment, plays a key role in virus evolution (Domingo et al., 2008; Domingo and Holland, 1997; Holland et al., 1991; Peñaranda et al., 2011), and which was primarily evaluated by determining the virus replication in the individual host (*in vivo*) or cell lines (*in vitro*) (Kurath, 2012), and virus strains with slower proliferation rates were considered to have lower adaptability than those replicate faster (Kim et al., 2023). A previous study found that IHN has different proliferation efficacy when cultured with various cell lines, such as EPC, RTG-2, and CHSE-214 cell lines, and showed different *in vivo* virulence in rainbow trout (Rodríguez et al., 2005). In this study, it was found that the IHN H202217 and IHN Sn1203 strain had the highest virus titer on EPC than on CHSE-214 and on RTG-2 cell lines, indicating that EPC was more sensitive than the other two cell lines, which was accordant with previous findings (Batts et al., 1991; Lorenzen et al., 1999; Wolf, 2019). However, the final titers of the IHN H202217 strain were

significantly lower than those of the IHN Sn1203 strain in the EPC and CHSE-214 cell lines, which indicating the IHN H202217 strain lost slightly propagation efficacy during evolution. We also detected the IHN H202217 strain with a polyclonal antibody against the G protein of IHN Sn1203 by using IFAT and found that it could be recognized by the antibody, indicating that although isolated from other fish it still maintains similar immunogenicity with that from rainbow trout.

IHN has been tested on fish within the genus *Salvelinus*, such as brook trout, lake trout, and Arctic charr. A Chinese J genogroup IHN strain was isolated from brook trout, but the virus strain was not artificially tested on brook trout (Jia et al., 2014), so we cannot know the lethality of the J IHN strain on brook trout. However, Bootland et al tested steelhead trout sourced IHN strain RB1 (U genogroup) and rainbow trout sourced IHN strain Rangen (type 2, genogroup unknown) on juvenile brook trout, and they found that the mortality rates were less than 35 % (Bootland et al., 1994). In addition, Follett et al challenged lake trout and Arctic charr with sockeye salmon sourced IHN, and a mortality rate of 15 % was observed on the lake trout, but IHN was undetectable in Arctic charr (Follett et al., 1997). However,



McAllister *et al* found that Arctic charr was susceptible to the rainbow trout sourced IHN strain, with a mortality rate of up to 41 %, and the prevalence of IHN in surviving fish is less than 24 % (McAllister *et al.*, 2000). In this study, we found both rainbow trout-sourced IHN and white-spotted charr-sourced IHN were less lethal to white-spotted charr but much higher lethal to rainbow trout, in which white-spotted charr sourced IHN caused lower mortality compared that caused by the rainbow trout-sourced IHN. These findings illustrated that the lethality of IHN to rainbow trout depends on the original source and fish species.

In the infection of IHN, the virus could be detectable in many organs, such as the liver, spleen, head kidney, brain, gills, intestines, and so on, especially in the spleen and head kidney (Chilmonczyk and Winton, 1994; Dixon *et al.*, 2016; Harmache *et al.*, 2006). Viral loads in tissue are an important index of viral proliferation, release, transmission, and adaptation, which has a close connection with lethality (Wargo *et al.*, 2016). Previous studies illustrated that IHN was initially detected in the gills of rainbow trout fry, followed by the liver, spleen, and head kidney, and finally in the brain (Brudeseth *et al.*, 2002; Drolet *et al.*, 1994; Yamamoto *et al.*, 1990; Yamamoto and Clermont, 1990). Similar dynamic distribution of the IHN H202217 and the IHN Sn1203 were observed when tested on rainbow trout (Fig. 8). However, the Sn1203 strain exhibited earlier virus emergence time and significantly higher viral loads than the H202217 in the majority of tissues from both alive and died rainbow trout, which could well explain the higher lethality of the IHN Sn1203 to rainbow trout than the IHN H202217 strain. Due to the low mortality of white-spotted charr after virus challenge, it is inadequate for statistical analysis of viral loads in dead fish, we only determined the viral loads in the alive white-spotted charr. We found that the IHN H202217 showed earlier virus emergence time and higher viral loads in white-spotted charr than IHN Sn1203, which suggests that the IHN H202217 has better fitness with the white-spotted charr than IHN Sn1203, while the IHN Sn1203 has better fitness with the rainbow trout than the IHN H202217.

We have a surveillance monitor on this fish farm where the H202217 was isolated for more than ten years, it was the first time to obtain IHN strain from white-spotted charr. Due to the co-cultivation of fish, the similar viral genogroup, and better fitness with white-spotted charr, we suspected that the IHN H202217 strain might be generated by host jumping during the evolution of local IHN strains. Based on these findings, combined with genome sequences of the IHN H202217, more attention should be paid to exploring the mechanism for IHN virulence evolution accompanied with host jumping, to provide prevention and control strategies for IHN disease in the future.

## 5. Conclusion

A novel IHN strain was first isolated and identified from white-spotted charr in China. Although sharing high genetic similarity to other Chinese J genogroup IHN strains, the novel IHN strain showed higher adaptability to the white-spotted charr than rainbow trout sourced IHN, and had moderate virulence to rainbow trout.

## Ethical approval

All experiments were conducted based on local government regulations, and fish experiments were approved by the Institutional Animal Care and Use Committee of Heilongjiang River Fisheries Research Institute, Chinese Academy of Fishery Sciences (20240506–001).

## Funding

This work was supported by Central Public-interest Scientific Institution Basal Research Fund, CAFS (HSY202301YB), Key R&D Program of Heilongjiang Province (2024ZXD38), Central Public-interest Scientific Institution Basal Research Fund, CAFS (NO. 2023TD45).

## CRedit authorship contribution statement

**Chunyan Guan:** Writing – review & editing, Writing – original draft. **Jingzhuang Zhao:** Supervision, Software, Conceptualization. **Yizhi Shao:** Software, Data curation. **Tongyan Lu:** Supervision, Conceptualization. **Liming Xu:** Writing – review & editing, Supervision, Funding acquisition.

## Declaration of competing interest

The authors declare that they have no known competing financial interests or personal relationships that could have appeared to influence the work reported in this paper.

## Appendix A. Supplementary data

Supplementary data to this article can be found online at <https://doi.org/10.1016/j.aquaculture.2025.742839>.

## Data availability

No data was used for the research described in the article.

## References

- Batts, W., Traxler, G., Winton, J., 1991. Factors Affecting the Efficiency of Plating for Selected Fish Rhabdoviruses.
- Bootland, L.M., Lorz, H.V., Rohovec, J.S., Leong, J.C., 1994. Experimental infection of brook trout with infectious hematopoietic necrosis virus types 1 and 2. *J. Aquat. Anim. Health* 6, 144–148. [https://doi.org/10.1577/1548-8667\(1994\)006<0144:EIOTW>2.3.CO;2](https://doi.org/10.1577/1548-8667(1994)006<0144:EIOTW>2.3.CO;2).
- Breyta, R., Black, A., Kaufman, J., Kurath, G., 2016. Spatial and temporal heterogeneity of infectious hematopoietic necrosis virus in Pacific northwest salmonids. *Infect. Genet. Evol.* 45, 347–358. <https://doi.org/10.1016/j.meegid.2016.09.022>.
- Brudeseth, B.E., Castric, J., Evensen, O., 2002. Studies on pathogenesis following single and double infection with viral hemorrhagic septicemia virus and infectious hematopoietic necrosis virus in rainbow trout (*Oncorhynchus mykiss*). *Vet. Pathol.* 39, 180–189. <https://doi.org/10.1354/vp.39-2-180>.
- OIE., 2021. Chapter 2.3.5: Infection with Infectious Hematopoietic Necrosis Virus. In: Manual of Diagnostic Tests for Aquatic Animals. <https://www.woah.org>.
- Chilmonczyk, S., Winton, J., 1994. Involvement of rainbow trout leucocytes in the pathogenesis of infectious hematopoietic necrosis. *Dis. Aquat. Org.* 19, 89–94. <https://doi.org/10.3354/dao019089>.
- Dale, O.B., Ørpetveit, I., Lyngstad, T.M., Kahns, S., Skall, H.F., Olesen, N.J., Dannevig, B.H., 2009. Outbreak of viral haemorrhagic septicaemia (VHS) in seawater-farmed rainbow trout in Norway caused by VHS virus genotype III. *Dis. Aquat. Org.* 85, 93–103. <https://doi.org/10.3354/dao02065>.
- Dixon, P., Paley, R., Alegria-Moran, R., Oidtmann, B., 2016. Epidemiological characteristics of infectious hematopoietic necrosis virus (IHN): a review. *Vet. Res.* 47, 63. <https://doi.org/10.1186/s13567-016-0341-1>.
- Domingo, E., Holland, J., 1997. RNA virus mutations and fitness for survival. *Ann. Rev. Microbiol.* 51, 151–178. <https://doi.org/10.1146/annurev.micro.51.1.151>.
- Domingo, E., Escarmís, C., Menéndez-Arias, L., Perales, C., Herrera, M., Novella, I.S., Holland, J.J., 2008. Viral quasispecies: dynamics, interactions, and pathogenesis. *Origin Evol. Viruses* 87. <https://doi.org/10.1016/B978-0-12-374153-0.00004-7>.
- Drolet, B.S., Rohovec, J.S., Leong, J.C., 1994. The route of entry and progression of infectious hematopoietic necrosis virus in *Oncorhynchus mykiss* (Walbaum): a sequential immunohistochemical study. *J. Fish Dis.* 17, 337–344. <https://doi.org/10.1111/j.1365-2761.1994.tb00229.x>.
- Duan, K., Zhao, J., Ren, G., Shao, Y., Lu, T., Xu, Lipu, Tang, X., Zhao, W., Xu, Liming, 2021. Molecular evolution of infectious pancreatic necrosis virus in China. *Viruses* 13, 488. <https://doi.org/10.3390/v13030488>.
- Einer-Jensen, K., Ahrens, P., Forsberg, R., Lorenzen, N., 2004. Evolution of the fish rhabdovirus viral haemorrhagic septicaemia virus. *J. Gen. Virol.* 85, 1167–1179. <https://doi.org/10.1099/vir.0.79820-0>.
- Enzmann, P.-J., Castric, J., Bovo, G., Thiery, R., Fichtner, D., Schütze, H., Wahli, T., 2010. Evolution of infectious hematopoietic necrosis virus (IHN), a fish rhabdovirus, in Europe over 20 years: implications for control. *Dis. Aquat. Org.* 89, 9–15. <https://doi.org/10.3354/dao02182>.
- Felsenstein, J., 1985. Confidence limits on phylogenies: an approach using the bootstrap. *Evolution* 39, 783–791. <https://doi.org/10.1111/j.1558-5646.1985.tb00420.x>.
- Follett, J.E., Meyers, T.R., Burton, T.O., Geesin, J.L., 1997. Comparative susceptibilities of salmonid species in Alaska to infectious hematopoietic necrosis virus (IHN) and north American viral hemorrhagic septicemia virus (VHSV). *J. Aquat. Anim. Health* 9, 34–40. [https://doi.org/10.1577/1548-8667\(1997\)009<0034:CSOSSI>2.3.CO;2](https://doi.org/10.1577/1548-8667(1997)009<0034:CSOSSI>2.3.CO;2).
- Garver, K.A., Batts, W.N., Kurath, G., 2006. Virulence comparisons of infectious hematopoietic necrosis virus U and M Genogroups in sockeye Salmon and Rainbow trout. *J. Aquat. Anim. Health* 18, 232–243. <https://doi.org/10.1577/H05-038.1>.

- Harmache, A., LeBerre, M., Droineau, S., Giovannini, M., Brémont, M., 2006. Bioluminescence imaging of live infected salmonids reveals that the fin bases are the major portal of entry for Novirhabdovirus. *J. Virol.* 80, 3655–3659. <https://doi.org/10.1128/JVI.80.7.3655-3659.2006>.
- He, M., Ding, N.-Z., He, C.-Q., 2021. Novirhabdoviruses versus fish innate immunity: a review. *Virus Res.* 304, 198525. <https://doi.org/10.1016/j.virusres.2021.198525>.
- Hoffmann, B., Beer, M., Schütze, H., Mettenleiter, T.C., 2005. Fish Rhabdoviruses: Molecular epidemiology and evolution. In: Fu, Z.F. (Ed.), *The World of Rhabdoviruses, Current Topics in Microbiology and Immunology*, vol. 292, pp. 81–117. [https://doi.org/10.1007/3-540-27485-5\\_5](https://doi.org/10.1007/3-540-27485-5_5).
- Holland, J.J., de la Torre, J.C., Clarke, D.K., Duarte, E., 1991. Quantitation of relative fitness and great adaptability of clonal populations of RNA viruses. *J. Virol.* 65, 2960–2967. <https://doi.org/10.1128/JVI.65.6.2960-2967.1991>.
- Huo, C., Ma, Z., Li, F., Xu, F., Li, T., Zhang, Y., Jiang, N., Xing, W., Xu, G., Luo, L., Sun, H., 2022. First isolation and pathogenicity analysis of a genogroup U strain of infectious hematopoietic necrosis virus from rainbow trout in China. *Transbound. Emerg. Dis.* 69, 337–348. <https://doi.org/10.1111/tbed.13983>.
- Jia, P., Zhu, X., Zheng, W., Zheng, X.C., Shi, X.J., Lan, W., Kan, S.F., Hua, Q.Y., Chen, X. X., 2013. Isolation and genetic typing of infectious hematopoietic necrosis virus from cultured brook trout (*Salvelinus fontinalis*) in China. *Bull. Eur. Assoc. Fish Pathol.* 33, 150–157.
- Jia, P., Zheng, X.-C., Shi, X.-J., Kan, S.-F., Wang, J.-J., He, J.-Q., Zheng, W., Yu, L., Lan, W.-S., Hua, Q.-Y., Liu, H., Jin, N.-Y., 2014. Determination of the complete genome sequence of infectious hematopoietic necrosis virus (IHN) Ch20101008 and viral molecular evolution in China. *Infect. Genet. Evol.* 27, 418–431. <https://doi.org/10.1016/j.meegid.2014.08.013>.
- Jia, P., Breyta, R.B., Li, Q., Qian, X., Wu, B., Zheng, W., Wen, Z., Liu, Y., Kurath, G., Hua, Q., Jin, N., Liu, H., 2018. Insight into infectious hematopoietic necrosis virus (IHN) in Chinese rainbow trout aquaculture from virus isolated from 7 provinces in 2010–2014. *Aquaculture* 496, 239–246. <https://doi.org/10.1016/j.aquaculture.2018.06.062>.
- Kim, S.Y., Kwak, J.S., Jung, W., Kim, M.S., Kim, K.H., 2023. Compensatory mutations in the matrix protein of viral hemorrhagic septicemia virus (VHSV) genotype IVa in response to artificial mutation of two amino acids (D62A E181A). *Virus Res.* 326. <https://doi.org/10.1016/j.virusres.2023.199067>.
- A, R., Kurath, G., 2012. Viral fitness: definitions, measurement, and current insights. *Curr. Opin. Virol.* 2, 538–545. <https://doi.org/10.1016/j.coviro.2012.07.007>.
- Kurath, G., Garver, K.A., Troyer, R.M., Emmenegger, E.J., Einer-Jensen, K., Anderson, E. D., 2003. Phylogeography of infectious hematopoietic necrosis virus in North America. *J. Gen. Virol.* 84, 803–814. <https://doi.org/10.1099/vir.0.18771-0>.
- Lorenzen, E., Carstensen, B., Olesen, N.J., 1999. Inter-laboratory comparison of cell lines for susceptibility to three viruses: VHSV, IHN and IPNV. *Dis. Aquat. Org.* 37, 81–88. <https://doi.org/10.3354/dao037081>.
- McAllister, P.E., Bebak, J., Wagner, B.A., 2000. Susceptibility of Arctic char to experimental challenge with infectious hematopoietic necrosis virus (IHN) and infectious pancreatic necrosis virus (IPNV). *J. Aquat. Anim. Health* 12, 35–43. [https://doi.org/10.1577/1548-8667\(2000\)012<0035:SOACTE>2.0.CO;2](https://doi.org/10.1577/1548-8667(2000)012<0035:SOACTE>2.0.CO;2).
- Niu, L., Zhao, Z., 1988. The epidemiology of IHN and IPN of rainbow trout in Northeast China. *J. Fish. China* 12, 327–332.
- Páez, D.J., LaDeau, S.L., Breyta, R., Kurath, G., Naish, K.A., Ferguson, P.F.B., 2020. Infectious hematopoietic necrosis virus specialization in a multihost salmonid system. *Evol. Appl.* 13, 1841–1853. <https://doi.org/10.1111/eva.12931>.
- Peñaranda, M.A.M.D., Wargo, A.R., Kurath, G., 2011. *In vivo* fitness correlates with host-specific virulence of infectious hematopoietic necrosis virus (IHN) in sockeye salmon and rainbow trout. *Virology* 417, 312–319. <https://doi.org/10.1016/j.virol.2011.06.014>.
- Raja-Halli, M., Vehmas, T.K., Rimaila-Pärnänen, E., Sainmaa, S., Skall, H.F., Olesen, N.J., Tapiovaara, H., 2006. Viral haemorrhagic septicaemia (VHS) outbreaks in Finnish rainbow trout farms. *Diseases of Aquatic Organisms* 72, 201–211. <https://doi.org/10.3354/dao072201>.
- Rodriguez, S., Alonso, M., Pérez-Prieto, S.I., 2005. Comparison of two birnavirus-rhabdovirus coinfections in fish cell lines. *Dis. Aquat. Org.* 67, 183–190. <https://doi.org/10.3354/dao067183>.
- Saitou, N., Nei, M., 1987. The neighbor-joining method: a new method for reconstructing phylogenetic trees. *Mol. Biol. Evol.* 4, 406–425. <https://doi.org/10.1093/oxfordjournals.molbev.a040454>.
- Tan, C.C.S., van Dorp, L., Balloux, F., 2024. The evolutionary drivers and correlates of viral host jumps. *Nat. Ecol. & Evol.* 8, 960–971. <https://doi.org/10.1038/s41559-024-02353-4>.
- Vakharia, V.N., Li, J., McKenney, D.G., Kurath, G., 2019. The nucleoprotein and phosphoprotein are major determinants of the virulence of viral hemorrhagic septicemia virus in rainbow trout. *J. Virol.* 93. <https://doi.org/10.1128/JVI.00382-19.e00382-19>.
- Wargo, A.R., Garver, K.A., Kurath, G., 2010. Virulence correlates with fitness in vivo for two M group genotypes of infectious hematopoietic necrosis virus (IHN). *Virology* 404, 51–58. <https://doi.org/10.1016/j.virol.2010.04.023>.
- Wargo, A.R., Scott, R.J., Kerr, B., Kurath, G., 2016. Replication and shedding kinetics of infectious hematopoietic necrosis virus in juvenile rainbow trout. *Virus Res.* 227, 200. <https://doi.org/10.1016/j.virusres.2016.10.011>.
- Wolf, K., 2019. Fish viruses and fish viral diseases. In: *Fish Viruses and Fish Viral Diseases*. Cornell University Press. <https://doi.org/10.7591/9781501746383>.
- Xu, L., Zhao, J., Liu, M., Kurath, G., Breyta, R.B., Ren, G., Yin, J., Liu, H., Lu, T., 2019. Phylogeography and evolution of infectious hematopoietic necrosis virus in China. *Mol. Phylogenet. Evol.* 131, 19–28. <https://doi.org/10.1016/j.ympev.2018.10.030>.
- Xu, L., Liu, M., Zhao, J., Ren, G., Dong, Y., Shao, Y., Lu, T., Zhang, Q., 2020. Infectious pancreatic necrosis virus inhibits infectious hematopoietic necrosis virus at the early stage of infection in a time dependent manner during co-infection in Chinook salmon embryo cell lines. *Fish Shellfish Immunol.* 102, 361–367. <https://doi.org/10.1016/j.fsi.2020.05.010>.
- Yamamoto, T., Clermont, T.J., 1990. Multiplication of infectious hematopoietic necrosis virus in rainbow trout following immersion infection: organ assay and Electron microscopy. *J. Aquat. Anim. Health* 2, 261–270. [https://doi.org/10.1577/1548-8667\(1990\)002<0261:MOIHNV>2.3.CO;2](https://doi.org/10.1577/1548-8667(1990)002<0261:MOIHNV>2.3.CO;2).
- Yamamoto, T., Batts, W.N., Arakawa, C.K., Winton, J.R., 1990. Multiplication of infectious hematopoietic necrosis virus in rainbow trout following immersion infection: whole-body assay and immunohistochemistry. *J. Aquat. Anim. Health* 2, 271–280. [https://doi.org/10.1577/1548-8667\(1990\)002<0271:MOIHNV>2.3.CO;2](https://doi.org/10.1577/1548-8667(1990)002<0271:MOIHNV>2.3.CO;2).